Received: 16, 19, 20 October, 2011
IOTC-2011-WPTT13-22

A Bayesian observation error model for otolith reading: The case study of yellowfin tuna (*Thunnus albacares*) in the Indian Ocean

Dortel E[1§], Massiot-Granier F[2§], Chassot E[1], Morize E[3], Million J[4], Hallier J-P[1], and Rivot E[2].

1 Institut de Recherche pour le Développement, UMR 212 EME (IRD-IFREMER-UM2), CRH, Avenue Jean Monnet, BP171, 34203 Sète Cedex, FRANCE

2 Agrocampus Ouest, UMR 985 ESE (INRA-Agrocampus Rennes), 65 rue de Saint Brieuc, CS 84215, 35042 Rennes cedex, FRANCE

3 Institut de Recherche pour le Développement, LEMAR, BP70, 29280 Plouzané, FRANCE

4 Indian Ocean Tuna Commission, PO Box 1011, Victoria, SEYCHELLES

Abstract

Growth curves are an essential input into the stock assessment of fish species. For yellowfin tuna, despite several studies conducted in the 3 oceans, based on tag-recapture experiments, length–frequency analyses data and direct ageing from calcified structures, the shape of the growth curve and its parameterization are still open to debate. In this study, a growth curve is derived using age estimates from the micro increments of sagittal otoliths from 179 yellowfin (19-135.4 cm FL). Otolith reading involves some subjective interpretation of the reader and entails different sources of uncertainty. Thus, an ageing error model that accounts for these uncertainties was developed. This model was then coupled with a Bayesian growth model that accounts for uncertainties in age estimation, individual variability in growth, and measurement errors and integrates expert knowledge. A VB log-K growth curve that allows a smooth transition between two different growth rate parameters was used. Results give a two-stanza growth pattern with a slow growth rate (2.38 cm mo^{-1}) up to around 67.5 cm FL, followed by a more rapid growth until 97 cm FL (4.24 cm mo^{-1}) before gradually decreasing. Our results are consistent with both those found in previous studies and with the biology of yellowfin. As a result, a new age-length key to update the conversion of catch-at-size into catch-at-age for future stock assessments of yellowfin is proposed.

Keywords: Age reading, Bayesian, growth, Indian Ocean, otolith, uncertainties, yellowfin

[§] The 2 first authors equally contributed to the manuscript

1. Introduction

Yellowfin tuna (*Thunnus albacares*) is an epipelagic species widely distributed in the tropical and subtropical waters of the major oceans. Its high economic value makes it the major target species for a wide variety of fishing fleets in the Indian Ocean (IO), from industrial fleets dominated by longline and purse seine to artisanal fleets, mainly using pole and line, driftnet, and hand line (Herrera & Pierre 2010). The total catch of yellowfin during 2001-2010 was about 380,000 t with Asian longliners (Japan, Taiwan- China and Korea) and European purse seiners representing 13% and 35% of the catch, respectively (IOTC, 2011). The artisanal fishery component of the IO is substantial, taking an estimated 35% of the total yellowfin catches during the 2000s but little accurate information is available on the fishing effort, location, and size structure of catch for most artisanal fisheries (Herrera & Pierre 2010)

Stock assessment for tuna stocks of the IO are conducted under the supervision of the Indian Ocean Tuna Commission (IOTC) and based on models incorporating knowledge about biological, ecological, and demographic processes on which the productivity of fish stocks and their resilience to fishing and environmental changes depend. The assessments remain complex due to our limited knowledge on the biological and ecological complexity of tunas, their highly migratory behavior, the particular characteristics of open-sea fisheries and the lack of data independent of commercial fisheries. To acquire such data and strengthen knowledge on tuna's population dynamics, an extensive tuna tagging project, funded by the European Union, was conducted in the Indian Ocean, between 2005 and 2007. The Regional Tuna Tagging Project (RTTP) was implemented by the Indian Ocean Commission (COI, www.coi-ioc.org/) and supervised by the IOTC. This project enabled to tag 168,164 tropical tunas, i.e. 32% yellowfin, 21% bigeye, and 47% skipkack. To date, 31,399 tagged tuna have been recaptured mainly by European purse seiners, and some recaptures of large individuals are expected in the forthcoming months and years.

Several studies have been conducted on the growth of yellowfin in the 3 oceans since the early 1960s based on mark-recapture experiments (Postel 1954, Fonteneau 1980, Bard 1984), analysis of changes in modes of catch derived from length–frequency data (Marcille & Stéquert 1976, Marsac & Lablache 1985, Marsac 1992), and direct ageing of otoliths (Le Guen & Sakagawa 1973, Uchiyama & Strushaker, 1981, Wild 1986, Morize 2008). Conflicting results due to differences in sampling, gear selectivity, and estimation methods historically raised issues about the shape of the growth curve and its parameterization. Some authors showed supporting evidence that yellowfin growth curve follows a Von Bertalanffy model which assumes a constant growth rate over the full lifespan of the individuals, implying a rapid growth of juveniles that continues through adulthood, slowly decreasing as the fish

approach their maximum size (Stéquert et al., 1996; Shuford et al. 2007). Conversely, more and more studies called this model into question and suggested a two-stanza growth curve with a significant change in growth rate between juveniles and adults (Fonteneau 1980, Gascuel et al., 1992 ; Lehodey & Leroy, 1999 ; Lumineau, 2002). Preliminary studies including both otolith and tag-recapture data collected throughout the RTTP-IO investigated different functional forms for the growth of yellowfin and clearly supported a two-stanza growth pattern for yellowfin characterized by a slowdown during their juvenile phase (Fonteneau & Gascuel, 2008; Eveson & Million 2008; Hillary et al. 2008; Morize et al., 2008).

Tag-recapture data have been widely used for modelling growth (Amstrup et al., 2005). The change in fish length between release and recapture provides valuable information about how individuals grow over time. Nevertheless, it does not provide information about the absolute age of fishes and auxiliary information is required to anchor the growth curve. Based on the tag-recapture data of the RTTP–IO and a starting point fixed at 33 cm for 0.5 years, Fonteneau and Gascuel (2008) derived an age-length key based on apparent average growth rates by 2 cm length classes. Based on this empirical age-length key, the values of the growth parameters of yellowfin were fixed in the 2010 stock assessment model (Langley et al. 2010). As underlined during the last WPTT, more work is however needed to achieve an appropriate integration of otolith and tagging data and agree on a growth model to be used in the assessment of the IO yellowfin stock.

Here, otolith data collected during the RTTP-IO were used within a consistent statistical framework to estimate the growth of yellowfin by taking into account all sources of uncertainties that are associated with measurements of length, time-at-liberty, and age derived from counts of otolith increments. Future work will focus on the combination of otolith, tag-recapture and length-frequency catch data in modeling tuna growth. Otolith data are a useful source of information on growth for species that consistently deposit growth increments over time because they provide a direct estimate of age (Panfili et al., 2002). However, otolith reading involves some subjective interpretation of reader and entails some uncertainties (Mariott & Mapstone, 2006; Punt et al., 2008). The first source of uncertainty comes from misinterpretations of reader that randomly occur. A second source of uncertainty often results from edge trimming during otolith preparation. A third source of uncertainty is a systematic bias on the exact fish birth date because the otolith nucleus is opaque and difficult to read. Moreover, the age of older fish is difficult to estimate because the increments are narrower and may overlap (Stéquert, 1995). On the other hand, growth increments are not consistently deposited daily, i.e. sub-daily increments and discontinuities in incrementation may occur (Panfili et al., 2002). It results in errors that influence estimates of biological parameters.

The objectives of the present study were (i) to develop an observation error model that accounts for the different sources of uncertainty in yellowfin age estimation, (ii) to develop a Bayesian growth estimation model that accounts for uncertainties in age estimation, individual variability in growth and measurement errors, and (iii) to propose a new age-length key so as to update the conversion of catch-at-size into catch-at-age for future stock assessments of yellowfin.

2. Materials

2.1. Tagging data

About 63,000 yellowfin were marked with conventional tags and released in the Western Indian Ocean between May 2005 and September 2007 through the RTTP-IO. Among them, 2,019 yellowfin were chemically tagged with oxytetracycline (OTC), an antibiotic that is incorporated and leaves a permanent fluorescent mark into calcified parts such as bones, scales, and otoliths. According to fish size, 1.5-3 mL of OTC were injected with a syringe in the intramuscular part of their back.

2.2. Otolith sampling, preparation and reading

Readings of daily otolith increments based on two distinct datasets. The first data set comes from the RTTP-IO project. 248 yellowfin chemically tagged have been recovered until now and 144 otoliths have been read, with size–at-tagging comprised between 43 and 111 cm fork length (FL) and size-at-recapture comprised between 47.9 and 135.4 cm FL. The second dataset comes from the West Sumatra Tuna Tagging Project (WSTTP) conducted in 2006-2007 by the IOTC and funded by the government of Japan. During this project, 35 otoliths of yellowfin were collected to provide additional information to the RTTP–IO data because they include small fishes, i.e. size comprised between 19 and 46.6 cm FL with 18 individuals of FL < 30 cm.

All otoliths collected were analysed at the "Laboratoire de Sclérochronologie des Animaux Aquatiques" (LASAA) in Brest, France. Otolith sagittae were prepared for age analysis following the methods described in Secor et al. (1991), Stéquert (1995), and Panfili et al. (2002). They were cleaned in sodium hypochlorite and rinsed with distilled water before being embedded in resin block and transversally cut on both sides of the nucleus. The section containing the nucleus was then fixed to a glass slide using thermoplastic glue and sanded to the level of the nucleus using different alumina grains (0.3 to 3 μm). The operation was performed on each side of the section until a slice of about 100 μm thickness was decalcified with EDTA (tri-sodium-ethylene-diaminetetraacetic acid) to increase contrast between increments. The thin slides were examined under a microscope (1000x magnification) for counting increments along the external part of the ventral side of sagitta. For the OTC tagged fishes, the number of increments was counted on different otolith sections: (i) between the nucleus and the OTC mark (*S1*), (ii) between the OTC mark and the edge (*S2*), and (iii) between the nucleus and the edge (*Stot*) (**Figure 1**). Otoliths from the WSTTP program were read in full (*Stot*).

Each otolith was read several times without prior knowledge on the size or time-at-liberty of the individuals sampled so as to maintain certain independence between the multiple readings, i.e. 1 to 3 times, 1 to 4 times and 1 to 5 times for *S1*, *S2*, and *Stot* respectively.

3. Coupling ageing error and growth models

3.1. Ageing error model

A hierarchical Bayesian model (Clark, 2005; Cressie et al., 2009) was used to exploit the information provided by the multiple readings of the same otolith as well as knowledge on other sources of uncertainty to quantify reading errors and uncertainty around age estimates.

A first model component, based on the subsample of tag-recapture data for OTC tagged fishes, was used to relate the counts of otolith increments after the OTC mark with the number of days between tagging and recapture (time-at-liberty; T_L) and validate the frequency of increment deposition. This model component was independently dealt with data selected for good reliability, i.e. individuals for which T_L was exactly known (i.e. knowledge on the accurate date of recapture) and for which the coefficient of variation of the different readings of a given otolith was inferior or equal to 10% (Marriott and Mapstone, 2006; Morize et al., 2008).

Under the hypothesis of daily increment formation (Wild & Foreman 1980; Wild et al., 1995) for otolith *i*:

(A.1) $$S2_{D\,i} = T_{L\,i}$$

Where $S2_{D\,i}$ is the number of deposited increments after the OTC mark. This number is known with uncertainties because some increments may be lost during the preparation of otolith and errors in interpreting and counting of rings can occur. These uncertainties were included from:

(A.2) $$S2_{D\,i} = S2_i + \psi_t$$

(A.3) $$S2^*_{i,\ell} \sim \mathcal{N}(S_i\,, {\varepsilon_{c\,i}}^2)$$

Where $S2^*_{i,\ell}$ is assumed to be the number of increments counted for reading ℓ of otolith i, ψ_t is the mean trimming error and $\varepsilon_{c\,i}$ is the reading error for otolith *i*. These errors tend to increase with age because the increments that are the furthest from the nucleus generally become narrower for old fishes and more difficult to distinguish (Stéquert, 1995). A multiplicative error was used to model this error process:

(A.4) $$\varepsilon_{c\,i} = CV \times S_i$$

Where the coefficient of variation (CV) is a measure of precision of different readings (Campana, 2001):

$$CV_i = 100 \times \frac{\sqrt{\frac{\sum_{\ell=1}^{R}\left(S^*_{i,\ell} - \bar{S}_i\right)^2}{R-1}}}{\bar{S}_i}$$

Where $\bar{S}_i$ is the average number of increments for otolith i.

From equations (A.1), (A.2) and (A.3), the following observation error model for the number of otolith increments was then proposed:

(A.5) $$S2_i = B \times T_{L\,i} - \psi_t$$

Where B represents the ratio between the number of increments and the T_L after considering the trimming error ψ_t. B should be close to 1 with few uncertainties (**Tables 1-3**).

The second model component utilizes the variability between multiple readings and results of the first component, i.e. the posterior distributions of B and ψ_t, as informative prior distributions, to estimate the age of each fish. The uncertainty around otolith readings (ε_c, ψ_t and nucleus bias ψ_n) was quantified to estimate the actual number of increments of each fish following a hierarchical structure similar to that described by equations A.2-A.3. Then this number of increments was converted to age by taking into account the frequency of increment deposition with respect to *S1* (age-at-tagging) and *S1*+T_L (age-at-recapture) (Eq. A.6-A.9 in **Table 2**) or, when *S1* was unknown or considered inaccurate, to *Stot*-T_L (age-at-tagging) and *Stot* (age-at-recapture) (Eq. A.10-A.13 in **Table 2**).

3.2. Validation of ageing error model by simulation

Different simulations were performed to test and validate the ageing error model proposed. The first simulation considered the various sources of uncertainty to evaluate the accuracy of the model and its relevance relative to the conventional method that is based on averaged ages. Additional simulations considering only the reading error were then performed with 4 or 10 readings of the same otolith to assess the model's ability to exploit information provided by the multiple readings. Accuracy of these estimates was assessed with the relative root mean square error (RMSE), a normalized indicator that measures the discrepancy between the simulated age and the estimated age. For each individual, the RMSE was calculated as follows:

$$RMSE = \frac{\sqrt{(A^* - A_a)^2}}{A^*}$$

Where A^* is the estimated age and A_a is the simulated age.

Simulated data sets contained 300 individuals, 150 individuals for which age was estimated from the number of increments between the nucleus and the fluorescent mark (*S1*) and 150 for which age was estimated from the total number of increments (*Stot*). The approach consisted in simulating realistic ages from which increment numbers considering B, ψ_t, ψ_n were then derived. The number of increments was then noisy by randomly generating repeated readings (**Figure 2**).

3.3. Two-stanza growth model

3.3.1. Model choice

An individual growth model describes the changes in size with age. Different functional forms of growth curve models have been proposed in the literature: Von Bertalanffy (1938), Gompertz (1825), Richards (1959), logistic (1975), generalized Von Bertalanffy (Pauly, 1979), Schnute-Richards (Schnute, 1990). However, these models do not seem appropriate for yellowfin tuna due to the succession of phases of acceleration and deceleration of growth. In this study, we considered the "VB log-K" model developed by Laslett et al. (2002) for the growth of southern bluefin tuna. This model is a continuous extension of the Von Bertalanffy model in which the growth rate coefficient *k* is modeled through a logistic function *k(t).* This function allows to take into account the existence of two different growth rate coefficients (k_1 and k_2) with a smooth transition between the two (Laslett et al., 2002, Eveson et al., 2004). The logistic function is given by:

(G.1) $$k(t) = k_1 + (k_2 - k_1) \times \frac{1}{1+\exp(-\beta\,(t - t_0 - \alpha))} \cong \begin{cases} k_1 & pour\ t \ll t_0 + \alpha \\ k_2 & pour\ t \gg t_0 + \alpha \end{cases}$$

Where α is the inflection point (relative mean age at which juveniles become adults) and β controls the rate of transition between k_1 and k_2, the transition being sharper for larger β (when $\beta \to \infty$, the change is abrupt). An advantage of the logistic form is that it can be explicitly integrated, yielding the growth curve:

(G.2) $$L(t) = L_{inf} \times \left(1 - exp\left(-k_2(t - t_0)\right) \times \left(\frac{1+exp\left(-\beta(t-t_0-\alpha)\right)}{1+exp(\beta\alpha)}\right)^{-(k_2 - k_1)/\beta}\right)$$

The VB log-K model was coupled with the ageing error model (**section 3.1**) to estimate the growth of yellowfin tuna. Let *i* the fish and *j* the opportunity of capture, equation (G.3) allows to join age-size individual observations with the mean state of the population, assuming that the entire variability comes from the measurement errors on the size of individuals (**Table 1**).

(G.3) $$L_{i,j} = L_{inf} \times \left(1 - exp\left(-k_2\left(A_{i,j} - t_0\right)\right) \times \left(\frac{1+exp\left(-\beta\left(A_{i,j}-t_0-\alpha\right)\right)}{1+exp(\beta\alpha)}\right)^{-(k_2 - k_1)/\beta}\right) + \varepsilon_{i,j}$$

Where $L_{i,j}$ is the length of fish *i* at age $A_{i,j}$ and A_{ij} was estimated by the ageing model error.

3.3.2. Estimate of growth parameters

The set of parameters $\theta = \{L_{inf}, k_1, k_2, \alpha, \beta, t_0\}$ and variance σ^2 were estimated by Bayesian fitting. In a Bayesian context, parameters θ are random variables for which a prior distribution $\pi(\theta)$ is assigned. This offers the possibility of introducing a priori information in the model from expert knowledge or analysis of external data. Bayes formula allows to update the prior distribution using the information provided by the data through the likelihood function to obtain a posterior distribution $\pi(\theta/L)$.

Estimate of the joint posterior distribution of the parameters was based on a MCMC (Monte Carlo Markov Chain) method using Gibbs sampler as implemented in OpenBugs.

Since the data set included little information on the asymptotic part of the growth curve, auxiliary information was provided for this parameter consistently with the available knowledge on the biology of the species. An informative prior distribution was defined for L_{inf} through the use of a generalized extreme value distribution (GEV), which allows extrapolation of the distribution tails behavior from the greatest values of a sample and thus estimates the occurrence probability of extreme events (Borchani, 2010). The distribution was fitted based on size measurement data (fork length) collected from the European purse seine fishery during fish processing at the IOT Ltd. cannery of Victoria, Seychelles, Maldivian pole and line vessels, and Taiwanese and Japanese longliners during 1952-2009 and available from the IOTC. The observed maximum fork length from each platform, fishery, and year was considered to represent *n* independent random variables $(L_1,\ldots,L_n)$ with common continuous distribution function F. Asymptotic length L_{inf} was then estimated from the approximation of the upper tail of $F(\ell)$ by using the $GEV_{\mu,\sigma,\xi}$ distribution:

$$GEV_{\mu,\sigma,\xi}(\ell) = \exp\left(-\left(1+\xi\left(\frac{\ell-\mu}{\sigma}\right)\right)^{-1/\xi}\right)$$

Where μ is a location parameter, σ is the scale parameter ($\sigma > 0$) and ξ is a tail index (shape parameter). The parameters of the $GEV_{\mu,\sigma,\xi}$ distribution were estimated by maximum likelihood method (**Table 3 and Figure 9**), i.e. estimating the values of the parameter vector $\theta=\{\mu, \sigma, \xi\}$ by minimizing the negative log-likelihood:

$$-LogV(\ell max,\theta) = -\sum_{i=1}^{n}\left(\left(\frac{1}{\sigma}\left(1+\xi\left(\frac{\ell max_i-\mu}{\sigma}\right)\right)^{-1-\xi/\xi}\exp\left(-\left(1+\xi\left(\frac{\ell max_i-\mu}{\sigma}\right)\right)^{-1/\xi}\right)\right)\right)$$

The priors of growth rate coefficients *k1* and *k2* were more difficult to define because they are specific to the VB log-K growth curve. Little informative priors were assigned to them. *k1* was assumed to vary according to a gamma prior distribution around a mean value determined from the literature based on growth curves derived from samples of fork length ≤ 75 cm (**Table 4**). $k2= k1+\kappa$ where κ follows a uniform prior distribution which is uninformative. Due to individual variability, α was assumed to be distributed around a mean age according to a normal distribution. Parameters of this distribution can be defined by literature, however α is a relative age depending on t_0. t_0 is a theoretical age that has no biological reality and greatly depends on the data. β is model-specific and no prior information was available in the literature. Therefore, we chose a uniform prior distribution for α and β parameters. Size measurement error ε was assumed to be distributed according to a normal prior

distribution around zero. The parameters of this distribution were determined from fishes of the RTTP-IO not marked with OTC and having a time-at-liberty inferior or equal to 10 days. These individuals were not included in subsequent analyses and therefore constitute an independent data set. Prior distributions are given in **Figure 3** and **Table 3**.

4. Results

4.1. Simulations

The variability in reading was shown to increase with the number of increments, justifying the use of a multiplicative error model (Eq. A4). The standard deviation in multiple readings of the same otolith increased with the average number of increments; the older a fish, the more the uncertainty around its age (**Figure 4**). Results of the first simulation indicated that the ageing error model was efficient in estimating the trimming bias (negative binomial posterior distribution similar to that simulated) despite the variability in simulated bias (from 0 to 8). The distribution of nucleus bias was not updated due to the fact that data contain no information to estimate this bias (mean simulated ψ_n= 16.94 increments and estimated ψ_n= 16.95 increments). The model overestimated *B* which was estimated at 0.99 while the simulated *B* was fixed to 0.96 (**Figure 5**).

The model provided age estimates more accurate than the conventional method. The average error derived from the RMSE was estimated to be 3.62% with the model against 6.66% for the conventional method (**Figure 6**). The RMSE values obtained with the model were significantly lower than those obtained with the conventional method (W=9375, *p-value* < 0.001 when the age was estimated from *S1*, W=9212, *p-value* <0.001 when the age was estimated from *Stot*).

Simulations focusing on the number of readings showed that the conventional method and ageing error models provided equivalent estimates of age (**Figure 7**). Using a Wilcoxon test, the RMSE values obtained with the model and the conventional method were not significantly different. Age estimates became more accurate when the number of readings increased.

4.2. Daily increment validation

The hypothesis of daily otolith increment was tested based on 24 yellowfin characterized by values of time-at-liberty comprised between 43 and 969 days (**Figure 8**). Mean posterior estimates derived from Bayesian fitting gave the following regression equation between the number of increments (*S2*) and time-at-liberty (T_L):

$$S2 = 0.99 \times T_L - 2.705$$

The marginal posterior probability distribution for *B* derived from MCMC outputs resulted in accepting the null hypothesis, confirming a daily otolith increment for yellowfin tuna (**Figure 5**).

4.3. Growth

The model supported a two-stanza growth for yellowfin with 2 distinct phases over the fish lifespan (**Figure 10**). The first stanza was characterized by a relatively slow growth, which gradually decreased to a minimum of 1.94 cm mo^{-1} up to 1.82 y (about 67.5 cm FL). This stanza was followed by a second stanza during which the growth accelerated up to a maximum of 7.08 cm mo^{-1} until 2.46 y (at about 97 cm FL) and then progressively decreased with size, becoming very slow when size was close to the asymptotic length (0.3 cm mo^{-1} at 151.5 cm FL) (**Figure 10** and **Table 6**). The average age at which juveniles became adults was estimated at 2.3 y, corresponding to about 84 cm FL. The growth parameters estimates are presented in **Table 5**.

4.4. Model fit and joint posterior distributions

Results from model fitting showed that some parameters were highly correlated. Strong positive correlation between k_1 and k_2 and negative correlation between growth rate coefficients and asymptotic length were found. Correlations resulted in some model instability and difficulty to estimate the posterior distribution for parameters β and k_2. Information provided through the prior distribution for L_{inf} compensated for the lack of information in the data set on large fishes (maximal fork length of 135.4 cm). The prior distribution of mean of 173.1 cm (**Figure 9**) was updated by the likelihood which resulted in a mean posterior estimate for L_{inf} of 153.6 cm FL. The growth curve derived from mean posterior estimates showed that all observations for fishes over 3 year-old were lower than predicted by the model. Otolith data collected on large yellowfin (up to 159 cm) within the RTTP-IO are currently being analysed at IRD and will be included in future growth estimation.

4.5. Sensitivity of fit to the data

The two tagging data sets provided complementary information. Data from the WSTTP provided information on young fishes (< 1 y) and greatly influenced the shape of the first part of the curve. Data from the RTTP-IO mainly provided information on fishes of intermediate size. The growth curve only fitted to the RTTP-IO data differed from the one fitted to all data (**Figure 12** and **Table 5**). The growth curve obtained from RTTP-IO data predicted a slower growth (k_1 and k_2 respectively estimated at 0.19 and 1.07 against 0.26 and 1.17 with all data). The growth rate reached a minimum of 1.45 cm mo^{-1} at 1.65 y (about 63.5 cm FL) and a maximum of 5.45 cm mo^{-1} to 2.29 y (about 86.4 cm FL). The average age at which juveniles become adults was estimated at 2.1 y and about 75 cm FL.

4.6. Age - length key

An age-length key was derived from results obtained with the VB log-K model (**Figure 14**). For an observed fork length L^*, the corresponded age was given by:

$$argmin\left(L^{*} - 153.6 \times \left(1 - exp\left(-1.172(A + 0.38)\right) \times \left(\frac{1 + exp\left(-11.07(A + 0.38 - 2.682)\right)}{1 + exp(11.07 \times 2.682)}\right)^{(0.263-1.172)/11.07}\right)\right)^{2}$$

5. Discussion

5.1. Ageing error model

Our results first confirm the deposit of daily growth increments in otoliths of yellowfin tuna that was observed in the Pacific Ocean (Wild and Foreman, 1980, Wild et al. 1995) and showed by Morize et al. (2008) on a subset of the data used in the present study. Conventional ageing methods based on averaging increment counts tends to underestimate the actual age of fishes since it generally neglects the nucleus part that is opaque and difficult to read and the possibility of edge trimming during otolith preparation. Our ageing error model aims to explicitly account for such potential biases so as to improve age estimation and propagate the uncertainty in increment reading as revealed by multiple readings. When considering only reading errors, simulations indicate that the model leads to similar results as for the conventional method. However, the model allows propagating the uncertainty in the age estimates while the conventional method only provides punctual estimates.

Although the model seems able to estimate the trimming bias that appears to be small (< 10 days) but variable between readings, it is unable to properly estimate the nucleus bias due to the lack of information in the data. This result confirms the usefulness of including expert knowledge on procedural errors in processing and interpreting otoliths. Bayesian analysis then appears particularly adapted to include auxiliary information in the statistical inference procedure. By contrast, simulations seem to indicate that the model is unable to estimate the frequency of increment formation. Additional simulations should confirm these results that might be due to the small number of replicates and help understand the source of bias in estimation. In any case, the recognition of bias improved significantly the age estimates showing the interest of the model as an alternative to the conventional method.

5.2. Yellowfin growth

Our results confirm that the VB log-K model is suitable for the growth of yellowfin tuna in the Indian Ocean while the Von Bertalanffy model resulted in growth overestimation for fishes ages 1-2 y and underestimation for individuals > 2 y (**Figure 13**). In absence of large fishes for which age estimates are available and despite information provided through prior distribution, the model seems to underestimate the expected asymptotic length of yellowfin estimated at about 153 cm FL. Based on size samples in the catch of the purse seiners and longliners, the mean asymptotic length would be around 175 cm FL, with maximum observed lengths of yellowfin up to 200 cm in the Indian Ocean. The maximum size reported for yellowfin tuna in the Atlantic Ocean is 239 cm FL (ICCAT, 2006). Sensitivity runs based on different prior distributions should be performed to assess the robustness of

the results. Future work will aim to include tag-recapture data from the RTTP-IO so as to provide information on growth rates of larger individuals and improve the estimation of yellowfin growth.

The results of this study confirm the hypothesis that yellowfin tuna in Indian Ocean shows a differential growth between juveniles and adults. The mean growth rates of smaller fisher (24 to 67.5 cm FL) and that of larger fishes (67.5 to 150 cm FL) are 2.38 cm mo^{-1} and 4.24 cm mo^{-1} respectively. Several studies based on tagging data, reading age of calcified structures (otoliths, spines, vertebrae, and scales) or length frequency analysis suggest a two stanza growth or at least the presence of an inflection point in the size/age curve. In the Indian Ocean, the initial growth rate was estimated at between 1.3 and 2.9 cm mo^{-1}, the fast growth rate of larger fishes being between 2.5 and 4.8 cm mo^{-1} (Marsac and Lablache, 1985; Anderson, 1988; Marsac, 1991; Firoozi and Carrara,1992 ; Lumineau, 2002) and the acceleration of growth occuring above 56-66 cm FL for Lumineau (2002), 62-66 cm FL for Marsac (1991) and 70 cm FL for Firoozi and Carrara (1992). Such results are consistent with those obtained in this study. The low growth rate for pre-adult yellowfin and the apparent acceleration of growth was also observed in the Atlantic and Pacific (Brouard et al., 1984; Wild, 1986; Gascuel et al., 1992; Lehodey and Leroy, 1999) oceans.

5.3. Which biological/ecological mechanisms behind the stanzas?

The variations in growth of yellowfin are linked to physiological, ecological and behavioral changes and remain poorly understood. The inflection point of the growth curve corresponds to a FL of about 75-84 cm for an age of about 2.2 y. According to Rohit & Rammohan (2009), the sex of yellowfin in the gonads is differentiated from 40 cm FL, first maturity is observed from 75-80 cm FL, and 50% of fishes reach maturity at 85-90 cm FL. Zudaire et al. (2010) estimated the length at which 50% of females reached sexual maturity at 77.8 cm FL in the Western Indian Ocean. For Bashmaker et al. (1991), the minimum FL at maturity for females is 52 cm. The inflection point appears to correspond to the mean fork length at which juveniles become adults, i.e. 50% of juveniles reached sexual maturity. The length from which growth accelerates, above 67.5 cm, could correspond to the minimum size of sexual maturity. Thus, the slowdown in growth during the first stanza would be related to the acquisition of sexual maturity. Growth rates depend on size, food consumption and metabolic rate (Walters & Essington, 2010). The ingested food provides a quantity of energy used by the fish first to maintain its metabolism and the excess of energy is used to its growth. The gonad maturation and development processes require a great amount of energy and causes a deficit of somatic growth. It is observed that bigger individuals have a relatively lower metabolic rate than small individuals. This variation of metabolic rate can be attributed, in part, to acquisition of sexual maturity but also to some physiological changes such as development of the swim bladder (Lehodey and Leroy, 1999; Lumineau, 2002). Yellowfin tunas have a small swim bladder, located in the viscera, which grows allometrically with fish size. This bladder is filled with oxygen, carbon dioxide, and nitrogen and it

has an important role to hydrostatic equilibrium of the fish. Until it attains about 50-60 cm, the fish has no gas in the bladder. As tunas have a density greater than seawater, then they must permanently swim to remain in the water. The larger yellowfin can adjust their buoyancy thanks to the swim bladder. Positive buoyancy allows them to remain in the water with an economy of movement. Negative buoyancy makes the swim "gliding" possible, which reduces drastically the energy required to swim and allows travel over longer distances and reach higher speeds (Magnuson, 1973). Furthermore, negative buoyancy allows them to make deeper dives.

Depending on age of yellowfin tunas, four types of diving behavior can be distinguished: surface-oriented, diving between the surface and 100 m, diving between the surface and 300 m and deep diving to over 500 m. According to a study of Schaefer et al. (2011) in the Pacific Ocean, dives from 50 to 300 m and deep dives are alternative foraging strategies for larger fishes. These authors estimated the minimum size of a fish exhibiting a deep dive at 60 cm FL, which corresponds to the size of the development of the swim bladder. The size at which growth accelerates (between 63.5 and 67.5 cm FL according to the data set) is close to this size. However, they attribute these diving abilities to the fact that the larger yellowfin have a higher physiological tolerance at lower temperatures and dissolved oxygen concentrations and can spend more time searching for prey at depths below the mixed layer. In conclusion, the development of the swim bladder associated with the increase in size and physiological changes may cause behavioral changes resulting in an extension of the habitat with potentially variations in food diet. The food diet changes and the migration of pre-adult yellowfin could have a great role in accelerating growth. It was observed that yellowfin juveniles (< 70 cm FL) tend to be concentrated in their nurseries, in the shallow and warm equatorial waters. Most of these young yellowfin are associated with small bigeye and skipjack in mixed species schools where intra and inter-specific competition is potentially high. The adults have a much larger geographical distribution and inhabit a wider range of colder waters (Fonteneau & Gascuel, 2008).

The growth model developed in this study provided information on the intrinsic growth parameters of yellowfin tuna, but it does not take into account environmental factors (temperature and food availability) that can influence growth nor provide information on the processes at the origin to the two stanzas. The estimate of somatic growth from otolith growth is a means to identify biological and ecological changes involved in the variation of growth and to estimate the age at which these changes occur. Constitutive proteins of otoliths are synthesized at the same rate as constitutive proteins of body tissues. This rate is controlled by endocrine endogenous rhythms and depends on food intake and temperature (Campana, 2001). Therefore, there is a relationship between otolith and somatic growth. However, the formation of the accretion zone that is composed of calcium carbonate is linked to physical chemistry processes and continues even when somatic growth is slowed or naturally stopped. Thus, the fishes having a slow growth have larger and heavier otoliths, relative to fish length, than

fishes having a faster growth (Mugiya and Tanaka, 1992; Panfili et al., 2002). Consequently, growth increments of otolith should enable to accurately identify the age at which the acceleration of growth occurs. Moreover, the observation of otolith increments allows estimating the age of first sexual maturity (Mollet et al. 2010). The process of gametogenesis uses both energy and reserves of calcium that could, in other circumstances, be allocated to otolith growth, which results in the presence of discontinuities of reproduction (Panfili et al., 2002). In addition, during its growth, the otolith incorporates some chemical elements of the environment. The strontium/calcium (Sr/Ca) ratio of the otolith has been shown to vary rapidly with salinity (Radtke 1989) and could be used to investigate changes in the habitat of juveniles and adult yellowfin related to vertical movements.

Acknowledgements. The tuna tagging data analysed in this publication were collected under the Indian Ocean Tuna Tagging Programme comprising the Regional Tuna Tagging Project of the Indian Ocean funded under the 9th European Development Fund (9.ACP.RSA.005/006) of the European Union, and several small-scale tagging projects funded by the European Union and the Government of Japan. We wish to acknowledge the contributions of all the people that have been involved in the Indian Ocean Tuna Tagging Programme. ED was supported by the EMOTION project through a grant from ORTHONGEL, the French Ministry of Agriculture and Fisheries (DPMA), and IRD. We are grateful to N Bousquet (EDF) for suggesting the use of GEV for modeling the prior distribution of asymptotic length and M Herrera (IOTC), C Assan (SFA), and Alicia Delgado de Molina (IEO) for data on yellowfin size measurements.

References

Amstrup S.C., McDonald T.L., Manly B.F.J. (2005) Handbook of capture-recapture analysis, *Princeton University Press*

Anderson R.C. (1988) Growth and migration of juvenile yellowfin tuna (*Thunnus albacares*) in the central Indian Ocean. *Coll. Vol. Work Doc.*, IPTP, TWS/88/21, p.28-39

Brouard F., Grandperrin R., Cillaurren E. (1984) Croissance des jeunes thons jaunes (*Thunnus albacares*) et des bonites (*Katsuwonus pelamis*) dans le Pacifique tropical occidental, *ORSTOM*, 24p.

Barde F.X. (1984) Croissance de l'albacore (*Thunnus albacares*) Atlantique d'après les données de marquages, *Coll. Vol. Sci. Pap. ICCAT* **20**(1), p.104-116

Campana S.E. (2001) Accuracy, precision and quality control in age determination, including a review of the use and abuse of age validation methods, *Journal of Fish Biology* **59**(2), p.197-242

Clark J.S. (2005) Why environmental scientists are becoming Bayesians. *Ecology letters* **8**, p.2–14

Cressie N., Calder C.A., Clark J.S., Hoef J.M., Wikle C.K. (2009) Accounting for uncertainty in ecological analysis: the strengths and limitations of hierarchical statistical modeling, *Ecological Applications* **19**, p.553–570

Essington T.E., Kitchell J.F., Walters C.J. (2001) The von Bertalanffy growth function, bioenergetics, and the consumption rates of fish. *Canadian Journal of Fisheries and Aquatic Sciences* **58**, p.2129-2138

Eveson P., Million J. (2008) Estimation of growth parameters for yellowfin, bigeye and skipjack tuna using tag-recapture data, *IOTC-2008-WPTDA-07*, 33p.

Eveson J.P., Laslett G.M., Polacheck T. (2004) An integrated model for growth incorporating tag–recapture, length–frequency, and direct aging data, *Canadian Journal of Fisheries and Aquatic Sciences* **61**, p.292-306

Firoozi A., Carrara G., (1992) An analysis of lengh-frequencies of *Thunnus albacares* in Iranian waters. *Coll. Vol. Work Doc.*, IPTP,TWS/92, p.95-102

Fonteneau A. (1980) Croissance de l'albacore (*Thunnus albacares*) de l'Atlantique Est, *Col. Vol. Sci. Pap. ICCAT* **9**(1), p.152-168

Fonteneau A., Gascuel D. (2008) Growth rates and apparent growth curves, for yellowfin, skipjack and bigeye tagged and recovered in the Indian Ocean during the IOTTP, IOTC-2008-WPTDA-08, 12p.

Gascuel D., Fonteneau A. & Capisano C., (1992) Modélisation d'une croissance en deux stances chez l'albacore (*Thunnus albacares*) de l'Atlantique Est, *Aquatic Living Resources* **5**, p.155-172

Hearn W.S., Polacheck T. (2003) Estimating long-term growth-rate changes of southern bluefin tuna (*Thunnus maccoyii*) from two periods of tag-return data, *Fishery Bulletin* **101**, p.58–74

Herrera M., Pierre L. (2010) Status of IOTC databases for tropical tunas, *IOTC-2010-WPTT-03*, 28p.

Hillary R.M., Million J., Anganuzzi A. (2008) Exploratory modelling of Indian Ocean tuna growth incorporating both mark-recapture data and otolith data, *IOTC-2008-WPTDA-03*, 10 p.

Langley A., Herrera M., Million J. (2010) Stock assessment of yellowfin tuna in the Indian Ocean using MULTIFAN-CL, *IOTC-2010-WPTT-23*, 72p.

Laslett G.M., Eveson J.P., Polacheck, T. (2002) A flexible maximum likelihood approach for fitting growth curves to tag–recapture data, *Canadian Journal of Fisheries and Aquatic Sciences* **59**, p.976-986

Le Guen J.C., Sakagawa G.T. (1973) Apparent growth of yellowfin tuna from the Eastern Atlantic ocean, *Fishery Bulletin* **71**(1), p.175-187

Lehodey P., Leroy B., (1999) Age and growth of yellowfin tuna (Thunnus albacares) from the western and central Pacific Ocean as indicated by daily growth increments and tagging data, *12th Meeting of the SCTB*, Standing Committee on Tuna and Billfish, Tahiti, p.1-21

Lumineau O. (2002) Study of the growth of Yellowfin tuna (Thunnus albacares) in the Western Indian Ocean based on length frequency data, *IOTC Proceedings* **5**, p.316-327

Magnuson J. J. (1973) Comparative study of adaptations for continuous swimming and hydrostatic equilibrium of scombroids and xiphoids fislies, *US Fishery Bulletin* **71**(2), p.337-356

Marcille J., Stéquert B. (1976) Etude préliminaire de la croissance du listao (*Katsuwonis pelamis*) dans l'ouest de l'océan Indien, *Cah. ORSTOM, Série Océanographique*, **14**(2), p.139-151

Marriott R.J., Mapstone B.D. (2006) Consequences of inappropriate criteria for accepting age estimates from otoliths, with a case study for a long-lived tropical reef fish, *Canadian Journal of Fisheries and Aquatic Sciences* **63**(10), p.2259-2274.

Marsac F., (1991) Growth of Indian Ocean Yellowfin Tuna estimated from size frequencies data collected on french purse seiners. *Coll. Vol.Work Doc.*, IPTP, TWS/91/17, p.35-39

Marsac F., Lablache G. (1985) Preliminary study of the growth of yellowfin estimated from purse seine data in the Western Indian Ocean, *Coll. Vol. Work Doc.*, IPTP, TWS/85/22, p.91-110

Mollet F.M., Ernande B., Brunel T., Rijnsdorp A.D. (2009) Multiple growth-correlated life history traits estimated simultaneously in individuals, *Oikos* **119**, p.10-26

Morize E., Munaron J.M., Hallier J.P., Million J. (2008) Preliminary growth studies of yellowfin and bigeye tuna (*Thunnus albacares* and *T. obesus*) in the Indian Ocean by otolith analysis, *IOTC Working Party on Tropical Tunas*, 13p.

Mugiya Y., Tanaka S. (1992) Otolith development, increment formation, and an uncoupling of otolith to somatic growth rates in larval and juvenile Goldfish, *Nippon Suisan Gakkaishi* **58**(5), p.845-851

Panfili J., De Pontual H., Troadec H., Wright P.J. (2002) Manuel de sclérochronologie des poissons, Eds. IFREMER-IRD, 464p.

Postel E. (1954) Deux allométries caractéristiques du thon à nageoires jaunes, *Neothunnus albacora* (Lowe) dans l'Atlantique tropico oriental, *Bulletin IFAN* **18**(1)

Punt A.E., Smith D.C., KrusicGolub K., Robertson S. (2008) Quantifying age-reading error for use in fisheries stock assessments, with application to species in Australia's southern and eastern scalefish and shark fishery, *Canadian Journal of Fisheries and Aquatic Sciences* **65**(9), p.1991-2005

Radtke R. L. (1989). Strontium-calcium concentration ratios in fish otoliths as environmental indicators. *Comparative Biochemistry* and *Physiology* **92**(A), p.189-193

Rohit P., Rammohan, K. (2009) Fishery and Biological Aspects of Yellowfin Tuna *Thunnus albacares* along Andhra Coast, India. *Asian Fisheries Science* **22**, p.235-244

Schaefer K.M., Fuller D.W., Block B.A. (2011) Movements, behavior, and habitat utilization of yellowfin tuna (*Thunnus albacares*) in the Pacific Ocean off Baja California, Mexico, determined from archival tag data analyses, including unscented Kalman filtering, *Fisheries Research*

Secor D.H., Dean J.M. & Laban E.H. (1991) Manual for otolith removal and preparation for microstructural examination, *Electric Power Research Institute and the Belle W. Baruch Institute for Marine Biology and Coastal Research*.

Shuford R.L., Dean J.M., Morize E. (2007) Age and growth of the yellowfin tuna in the Atlantic Ocean, *Collective Volume of Scientific Papers ICCAT* **60**(1), p.330-341

Stéquert B., (1995) Détermination de l'âge des thons tropicaux à partir de leurs otolithes : exemple du Yellowfin (*Thunnus albacares*), *Document Technique du Centre ORSTOM de Brest* **76**, p.1-31

Stéquert B., Rodriguez J.N., Cuisset B., Le Menn F. (2001) Gonadosomatic index and seasonal variations of plasma sex steroids in skipjack tuna (*Katsuwonus pelamis*) and yellowfin tuna (*Thunnus albacares*) from the western Indian ocean, *Aquatic Living Resources* **14**, p.313-318

Stéquert B., Panfili J., Dean J.M. (1996) Age and growth of yellowfin tuna, *Thunnus albacares*, from the western Indian Ocean, based on otolith microstructure, *Fishery Bulletin* **94**, p.124–134

Uchiyama J.H., Struhsaker P. (1981) Age and growth of skipjack tuna, *Katsuwonus pelamis*, and yellowfin tuna, *Thunnus albacares* as indicated by daily growth increments of sagittae. *Fishery Bulletin* **79**, p.151-162

Walters C., Essington T. (2010) Recovery of bioenergetics parameters from information on growth: overview of an approach based on statistical analysis of tagging and size-at-age data, *The Open Fish Science Journal* **3**, p.52-68

Wang Y.G. (1998) Growth curves with explanatory variables and estimation of the effect of tagging, *Australian & New Zealand Journal of Statistics* **40**(3), p.299-304

Wild A. (1986) Growth of yellowfin tuna, *Thunnus albacares*, in the Eastern Pacific Ocean based on otolith increments, *Inter-American Tropical Tuna Commission Bulletin* **18**(6), p.423-479

Wild A., Foreman T.J. (1980) The relationship between otolith increments and time for yellowfin and skipjack tuna marked with tetracycline, *Inter-American Tropical Tuna Commission Bulletin* **17**(7), p.507-560

Wild A., Wexler J.B., Foreman T.J. (1995) Extended studies of increment deposition rates in otoliths of yellowfin and skipjack tunas, *Bulletin of Marine Science* **57**(2), p. 555-562

Zudaire I., Murua H., Grande M., Korta M., Arrizabalaga H., Areso J., Delgado-Molina A. (2010) Reproductive biology of yellowfin tuna (*Thunnus albacares*) in the Western and Central Indian Ocean, IOTC-2010- WPTT-48, 25p.

Table 1. Parameters and variables used in ageing error and growth models

Notation	Definition	Equation
$S2_D$	Number of increments deposited between OTC mark and edge	A.2
$S2$	Number of increments counted between OTC mark and edge	A.2 and A.3
$S2^*$	Number of increments deposited between OTC mark and edge	A.3
T_L	Number of days between tagging and recapture	A.5, A.9 and A.10
B	Ratio between the number of increments and T_L	A.5, A.8, A.12
ψ_t	Trimming bias	A.5, A.10
ψ_n	Nucleus bias	A.6, A.10
ε_c	Reading errors	A.4
A_t	Age-at-tagging	A.8 and A.13
A_r	Age-at-recapture	A.9 and A.12
$S1_D$	Number of increments deposited between nucleus and OTC mark	A.6
$S1$	Number of observable increments between nucleus and OTC mark	A.6 and A.7
$S1^*$	Number of increments counted between nucleus and OTC mark	A.7
$Stot_D$	Total number of increments deposited	A.10
$Stot$	Total number of increments observable	A.10 and A.11
$Stot^*$	Total number of increments counted	A.11
L_{inf}	Asymptotic fork length	G.2 and G.3
k_1	Juvenile growth rate coefficient	G.2 and G.3
k_2	Adult growth rate coefficient	G.2 and G.3
α	Relative inflection point	G.2 and G.3
β	Transition rate	G.2 and G.3
t_0	Theoretical age at fork length 0	G.2 and G.3
ε	Length measurement error	G.3

Table 2. Ageing error model equations

Deterministic equations		Stochastic equations	
(A.2)	$S2_{D\,i} = S2_i + \psi_t$	(A.3)	$S2^*_{i,\ell} \sim \mathcal{N}(S_i\,, {\varepsilon_c}_i^2)$
(A.5)	$S2_i = B \times T_{L\,i} - \psi_t$		
(A.6)	$S1_{D\,i} = S1_i + \psi_n$	(A.7)	$S1^*_{i,\ell} \sim \mathcal{N}(S1_i\,, {\varepsilon_c}_i^2)$
(A.8)	$A_{t\,i} = \frac{1}{B} \times S1_{D\,i}$		
(A.9)	$A_{r\,i} = A_{t\,i} + T_{L\,i}$		
(A.10)	$Stot_{D\,i} = S1_i + \psi_n + \psi_t$	(A.11)	$Stot^*_{i,\ell} \sim \mathcal{N}(Stot_i\,, {\varepsilon_c}_i^2)$
(A.12)	$A_{r\,i} = \frac{1}{B} \times Stot_{D\,i}$		
(A.13)	$A_{t\,i} = A_{r\,i} - T_{L\,i}$		

Table 3. Priors on the ageing and growth parameters

Ageing parameter	**Prior distribution**	**Prior distribution parameter**
B	$B' \sim Beta(a,b)\,; B = 2 \times B'$	$a = b = 1$
ψ_t	${\psi_t}' \sim Beta(a,b)\,; \psi_t = 10 \times {\psi_t}'$	$a = b = 1$
ψ_n	$\psi_n \sim \mathcal{N}(\mu_n, {\sigma_n}^2)$	μ_n = 17 σ_n = 2
Growth parameter	**Prior distribution**	**Prior distribution parameter**
L_{inf}	$GEV_{\mu,\sigma,\xi}(\ell) = \exp\left(-\left(1+\xi\left(\frac{\ell-\mu}{\sigma}\right)\right)^{-\frac{1}{\xi}}\right)$	μ=173.141 σ=11.067 ξ=-0.3474
k_1	Gamma distribution $\Gamma(a,b)$	μ_k = 0.64 CV_k = 0.3
k_2	$k_1 + \kappa \quad \kappa \sim U(min_\kappa, max_\kappa)$	min_κ = 0 max_κ = 3
A	Normal distribution $\mathcal{N}(\mu_\alpha, {\sigma_\alpha}^2)$	μ_α = 2.5 σ_α = 0.5
t_0	Uniform distribution $U(min_{t0}, max_{t0})$	min_{t0} = -2 max_{t0} = 0
β	Uniform distribution $U(min_\beta, max_\beta)$	min_β = 0 max_β = 20
ε	Normal distribution $\mathcal{N}(\mu_\varepsilon, \sigma^2)$	μ_ε = 0 σ = 1.14

Table 4. Growth rate coefficients of yellowfin tuna in the three oceans

Ocean	Data	Method	Growth rate coefficient	Length range (cm)	Reference
Western Indian	Length-frequencies	Von Bertalanffy	0.88	< 60	Lumineau (2002)
			0.8		
		Gascuel model	0.84		
			0.192		Cayré and Ramcharrun (1990)
Atlantic	Otoliths	Von Bertalanffy	0.281	30-179	Shuford et al. (2007)
	Length-frequencies	Von Bertalanffy	0.42	63-150	Gascuel et al. (1992)
		Gascuel model	1.195	40-150	
Western Pacific	Otoliths	Von Bertalanffy	0.39	45-70	Lehodey and Leroy (1999)
		Modified Von Bertalanffy	0.728 males: 0.805 females: 0.511		

Table 5. Estimated parameters of the growth model coupled with ageing error model according to the two data sets (sd = Standard error)

Parameters		**RTTP data**		**All data**	
		Mean	**sd**	**mean**	**sd**
Fork asymptotic length	L_{inf} (cm)	153.1	18.12	153.6	18.99
Juvenile growth rate coefficient	k_1	0.19	0.042	0.263	0.051
Adult growth rate coefficient	k_2	1.066	0.631	1.172	0.7
Relative inflection point	α (year)	3.27	0.372	2.682	0.33
Transition rate	β	11.78	4.623	11.07	5.099
Theorical age at fork length 0	t_0 (year)	-1.17	0.344	-0.38	0.102
Measurement error	ε (cm)	1.33	0.006	1.142	0.006

Table 6. Estimated monthly growth rate of yellowfin according to all data

Fork length (cm)	**Average growth rate (cm mo^{-1})**
24-30	2.775
30-40	2.602
40-50	2.383
50-60	2.163
60-67.5	1.983
67.5-70	1.950
70-84	3.137
84-96	6.635
96-110	6.685
110-120	5.459
120-130	4.071
130-140	2.610
140-150	1.082

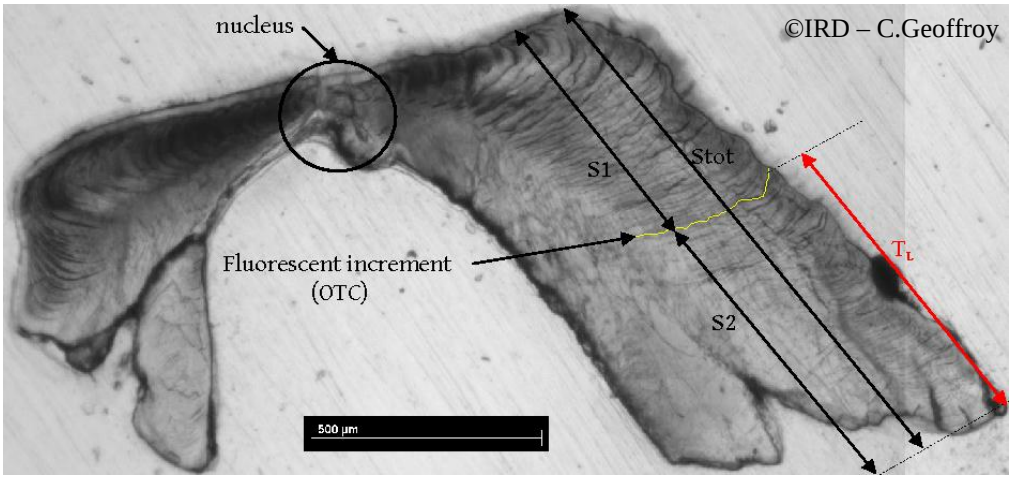

Figure 1. Otolith of yellowfin tuna showing the different sections used for reading the number of increments. OTC = Oxytetracycline; S1 = section from the nucleus to the OTC mark; S2 = section from the OTC mark to the otolith edge; T_L: Time-at-Liberty (© IRD - C. Geffroy)

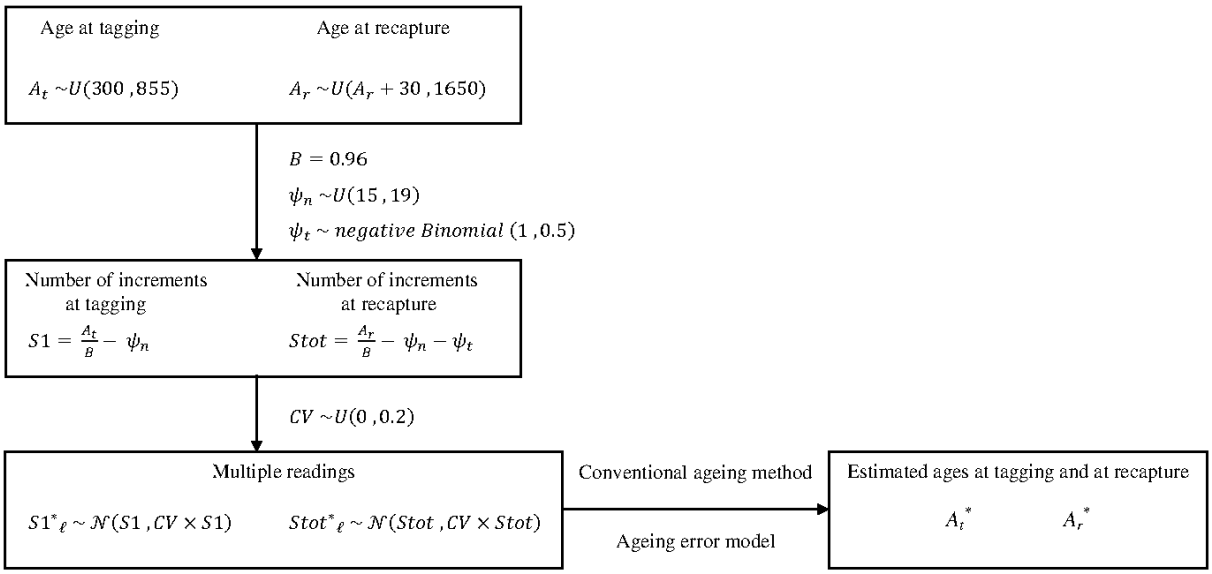

Figure 2. Simulation framework for testing the ageing error model. Different sources of uncertainty are added to simulated ages to randomly generate noisy increments that were then used as inputs in the model

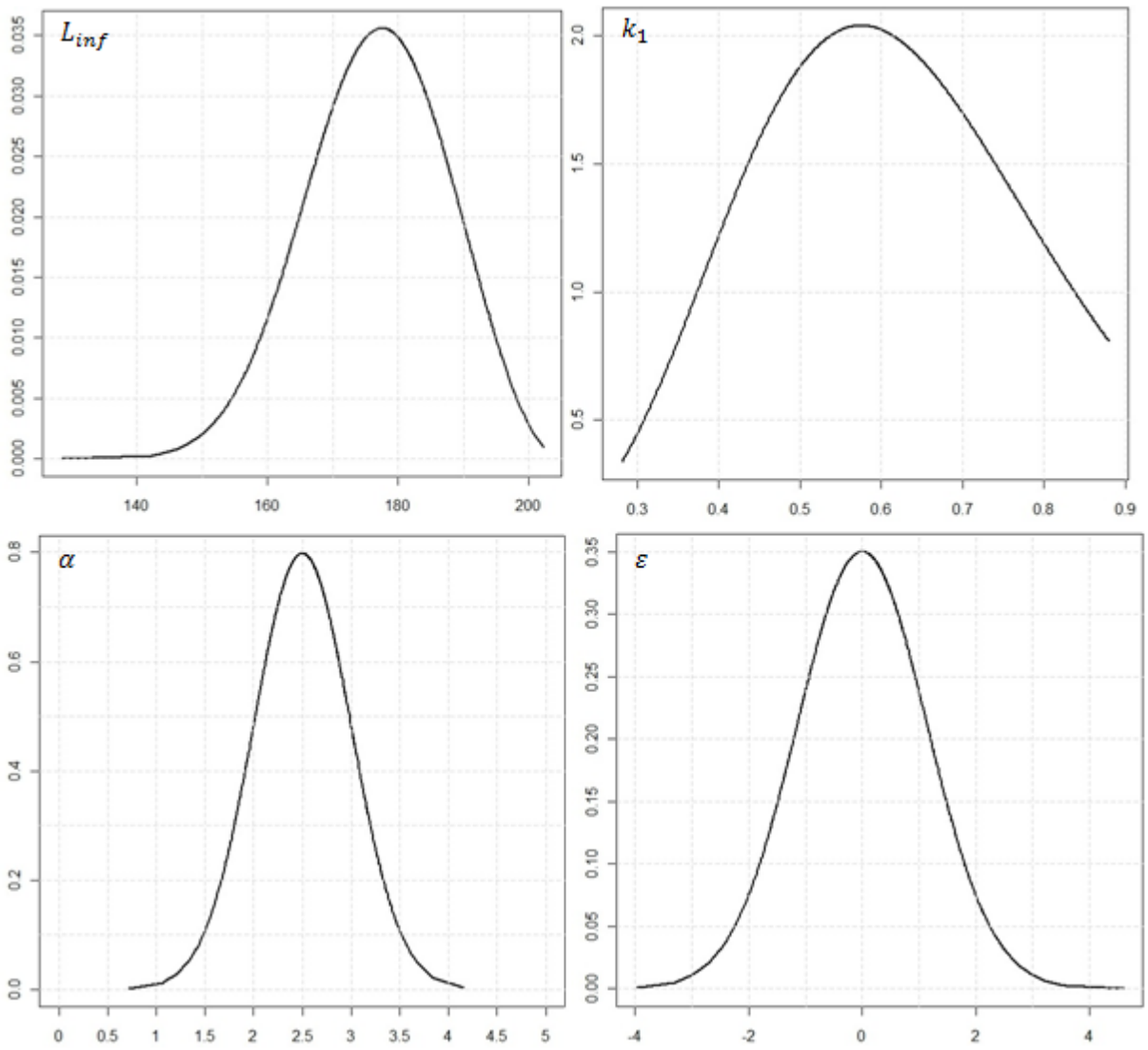

Figure 3. Prior distributions of growth parameters. L_{inf}.: asymptotic length (cm), k_1: growth rate coefficient of the first life phase, α: inflection point (years), ε: length measurement error (cm)

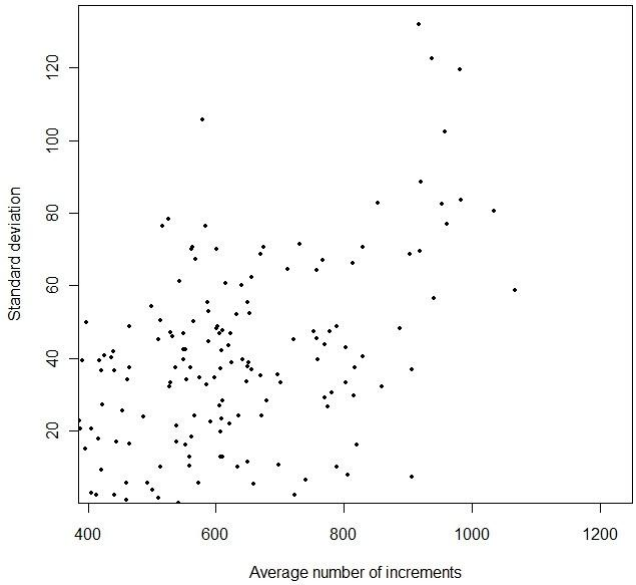

Figure 4. Evolution of the standard deviation of multiple readings of otoliths as a function of the average number of increments

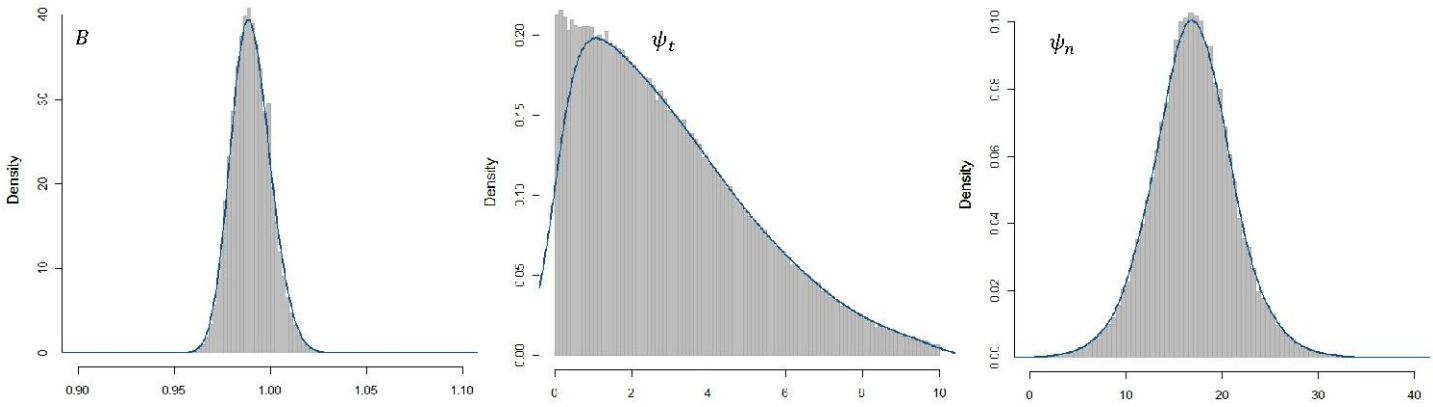

Figure 5. Marginal posterior distributions for the parameters of the ageing error model. B = ratio between number of increments and number of days-at-sea; ψ_n = error on the nucleus; ψ_t = Error on the terminal part (edge) of the otolith

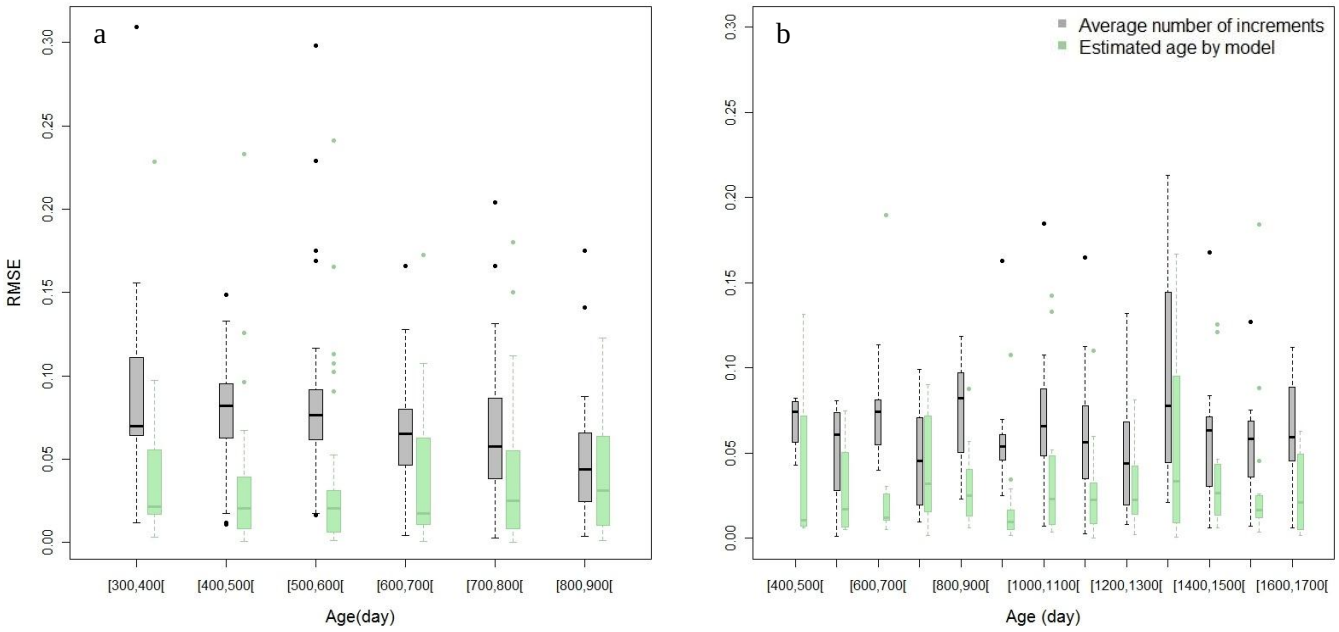

Figure 6. Boxplot of the relative mean square error (RMSE) of estimated age by ageing error model and conventional method from *S1* (a) and *Stot* (b) conditionally to the simulated age

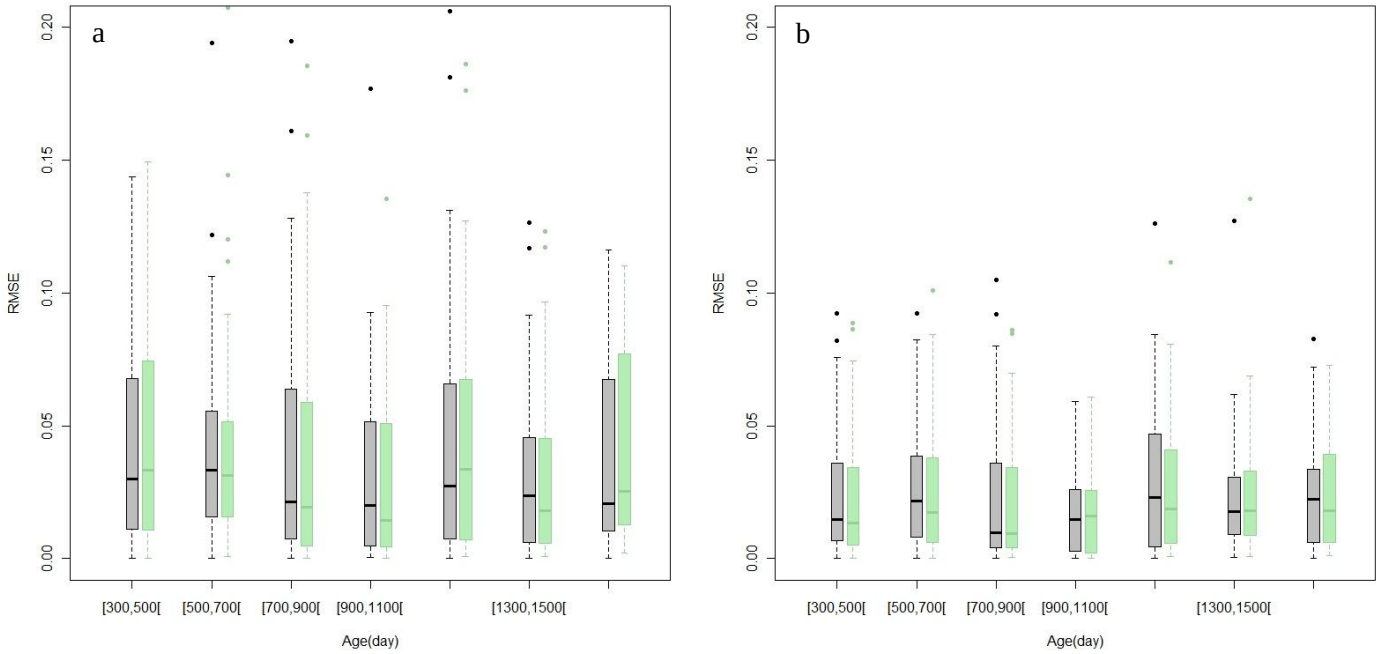

Figure 7. Boxplot of the relative mean square error (RMSE) of estimated age by ageing error model and conventional method for four (a) and ten (b) readings

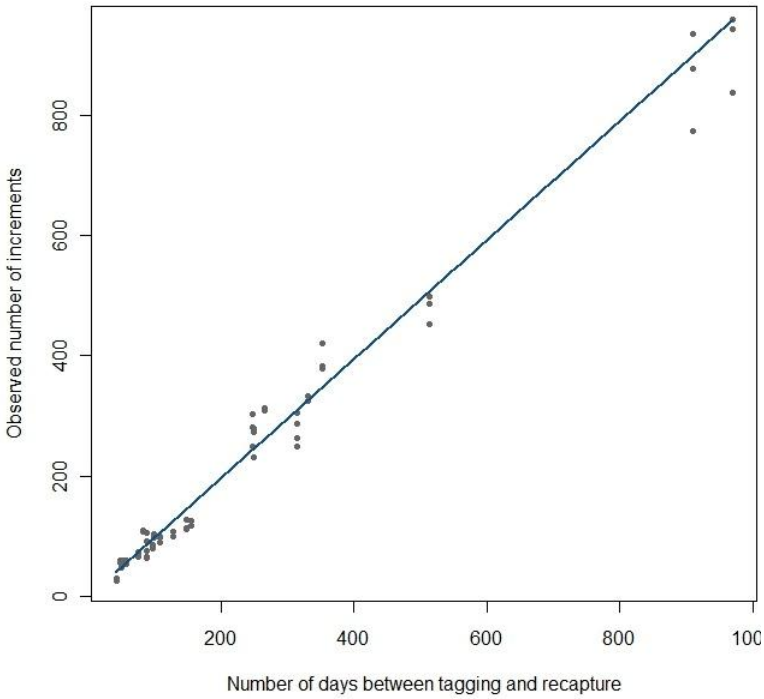

Figure 8. Relationship between the number of increments deposited after the OTC mark (*S2*) and the number of days-at-liberty (T_L)

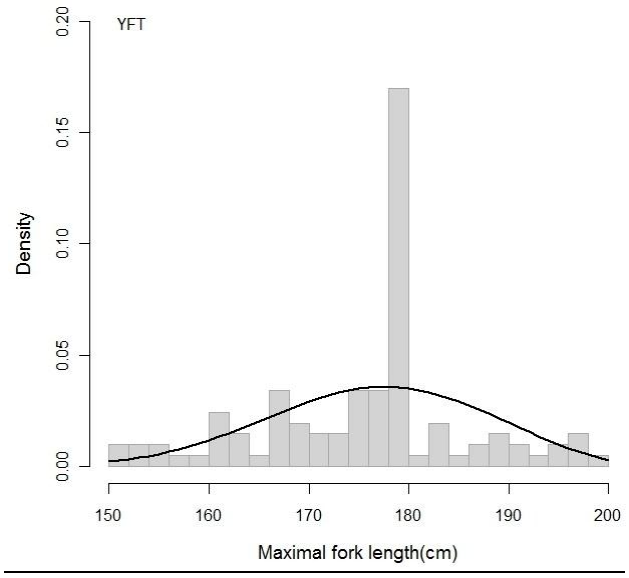

Figure 9. Distribution of observed maximal fork lengths and fitting of density of $GEV_{\mu,\sigma,\xi}$

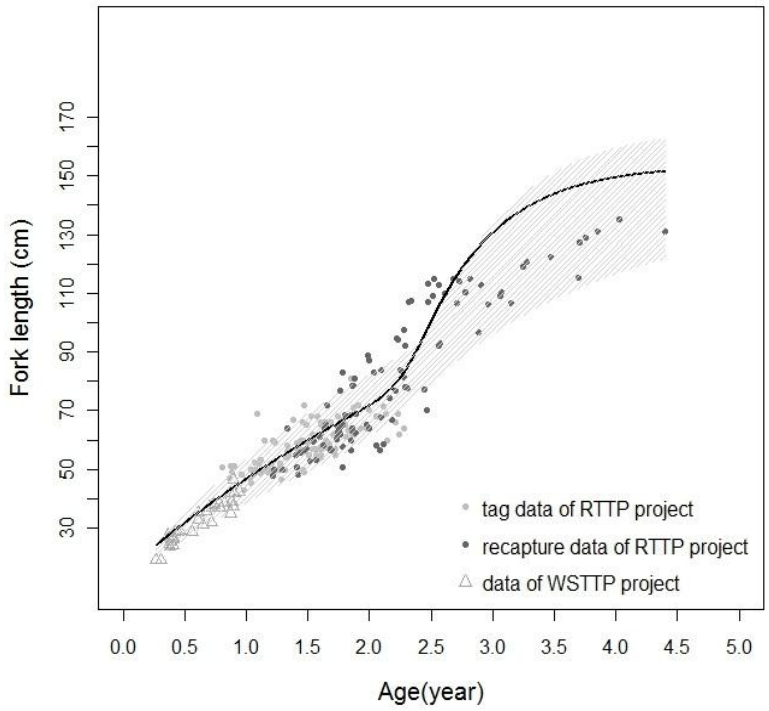

Figure 10. Yellowfin growth curve as estimated from the VB log-K model coupled with ageing error model and 25% and 75% quartiles

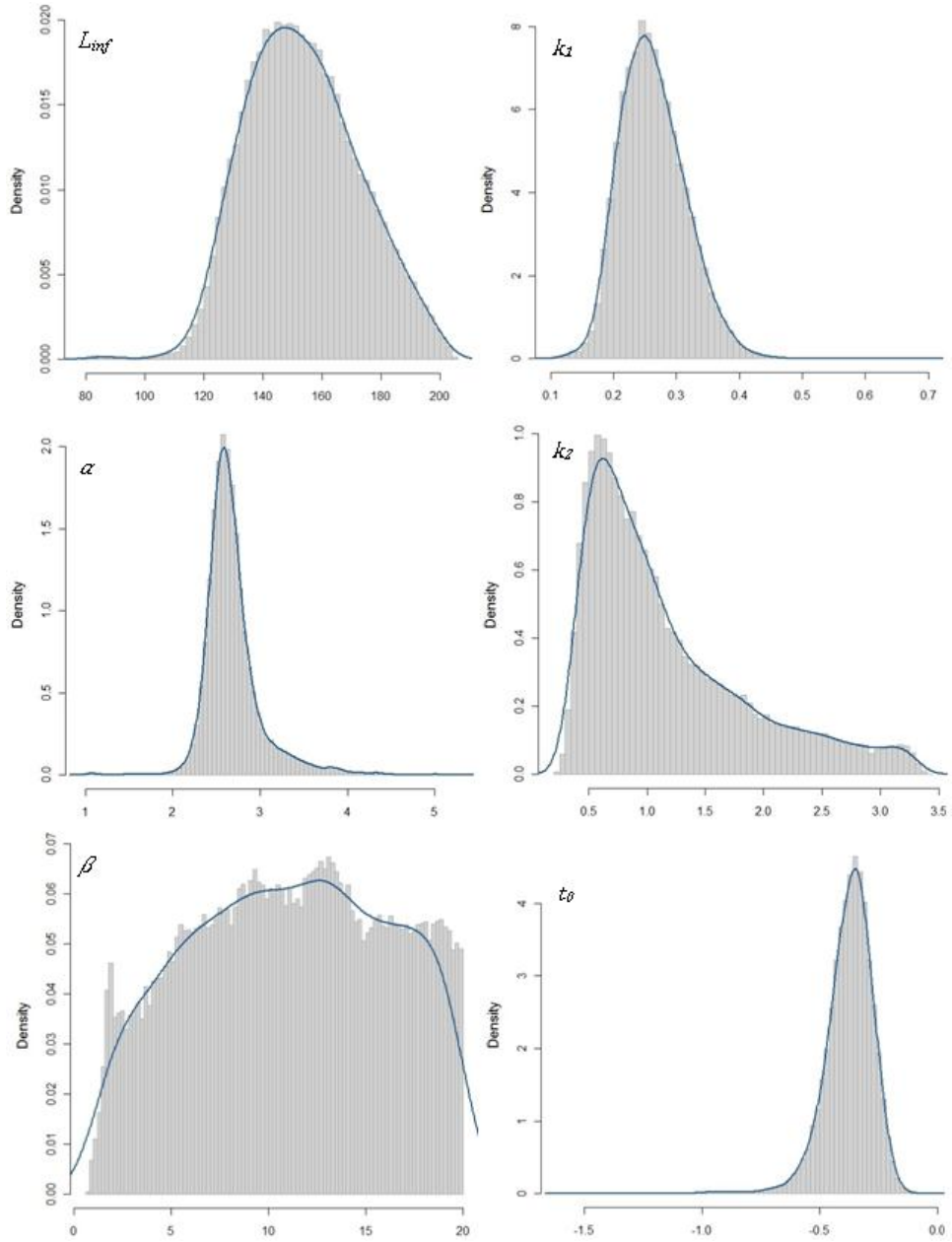

Figure 11. Marginal posterior distributions of growth parameters

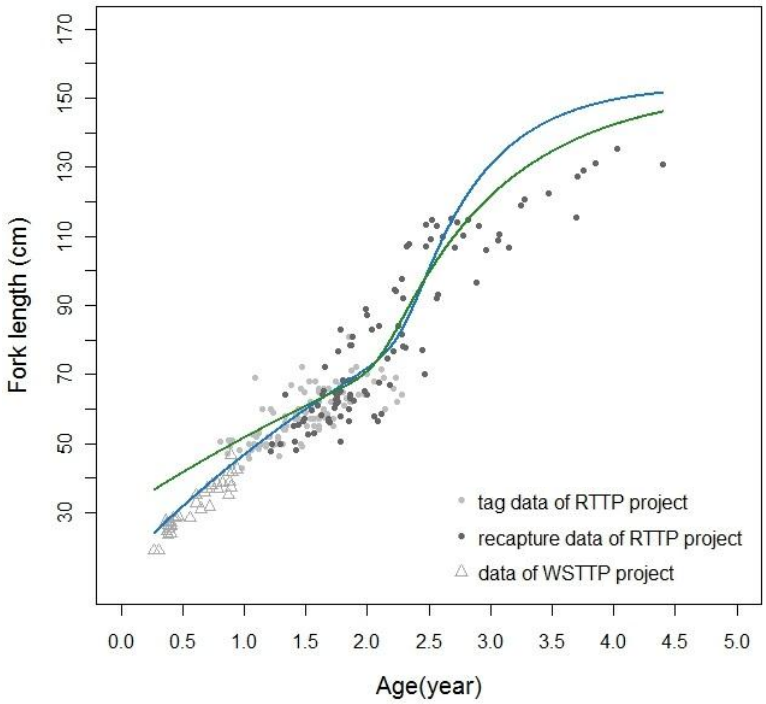

Figure 12. Yellowfin growth curve according to all data (blue) and data from RTTP-IO (green)

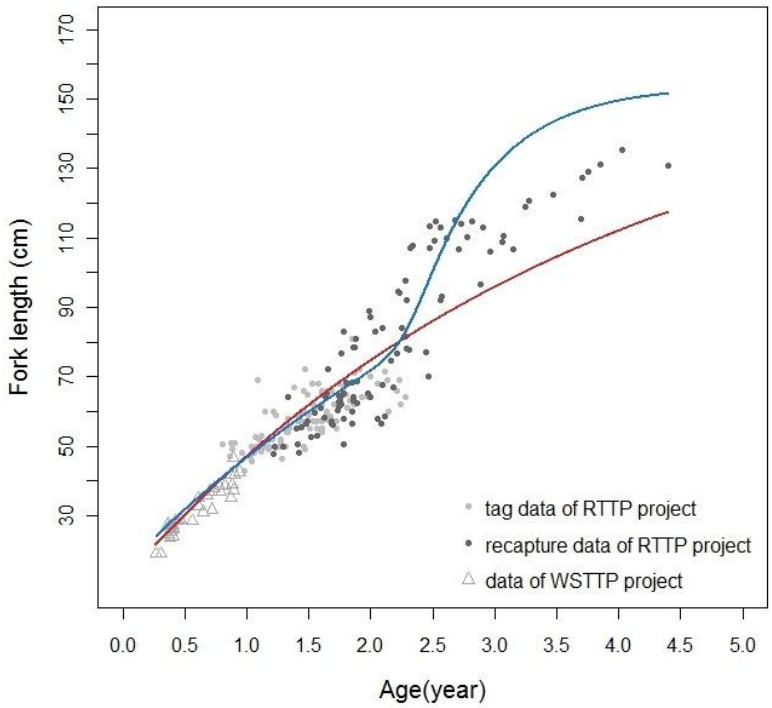

Figure 13. Yellowfin growth curve according to Von Bertalanffy model (red) and Von Bertalanffy log-K model (blue)

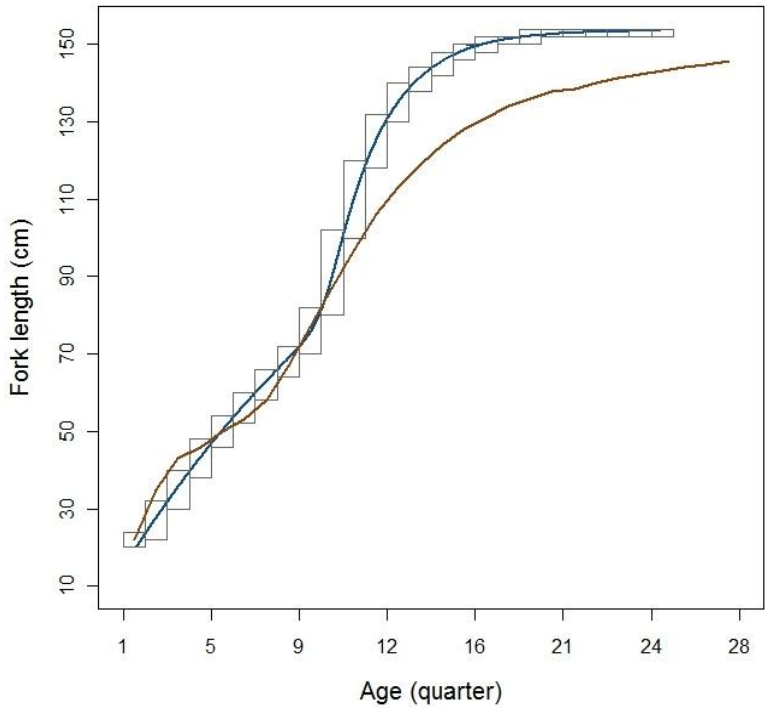

Figure 14. Comparison between (blue) the growth model fitted to all data with corresponding length-age-length key based on slicing and (brown) the growth of yellowfin currently used in the 2011 stock assessment model (Fonteneau and Gascuel, 2008)